Elsevier Editorial System(tm) for Geochimica et Cosmochimica Acta

Manuscript Draft

Manuscript Number:

Title: The stoichiometric dissociation constants of carbonic acid in seawater brines from 298 to 267 K

Article Type: Article

Corresponding Author: Dr. Stathys Papadimitriou, Ph.D.

Corresponding Author's Institution: Bangor University

First Author: Stathys Papadimitriou, Ph.D.

Order of Authors: Stathys Papadimitriou, Ph.D.; Socratis Loucaides, Ph.D.; Victoire Rérolle, Ph.D.; Paul Kennedy, B.Sc.; Eric P Achterberg, Ph.D.; Andrew G Dickson, Ph.D.; Matthew Mowlem, Ph.D.; Hilary Kennedy, Ph.D.

Abstract: The stoichiometric dissociation constants of carbonic acid (K1C* and K2C*) were determined by measurement of all four measurable parameters of the carbonate system (total alkalinity, total dissolved inorganic carbon, pH, and CO2 fugacity) in natural seawater and seawater-derived brines, with a major ion composition equivalent to that of Standard Reference Seawater, to practical salinity (SP) 100 and from 25 °C to the freezing point of these solutions and -6 °C temperature minimum. These values, reported in the total proton scale, provide the first such determinations at below-zero temperatures and for SP > 50. The temperature (T, in Kelvin) and SP dependence of the current pK1C* and pK2C* (as negative common logarithms) within the salinity and temperature ranges of this study (33 ≤ SP ≤ 100, -6 °C ≤ t ≤ 25 °C) is described by the following best-fit equations: pK1C* = -176.48 + 6.14528×SP^0.5 - 0.127714×SP + 7.396×10^-5×SP^2 + (9914.37 - 622.886×SP^0.5 + 29.714×SP)×T^-1 + (26.05129 - 0.666812×SP^0.5)×lnT (σ = 0.011, n = 62), and pK2C* = -323.52692 + 27.557655×SP^0.5 + 0.154922×SP - 2.48396×10-4×SP^2 + (14763.287 - 1014.819×SP^0.5 - 14.35223×SP)×T^-1 + (50.385807 - 4.4630415×SP^0.5)×lnT (σ = 0.020, n = 62). These functions are suitable for application to investigations of the carbonate system of internal sea ice brines with a conservative major ion composition relative to that of Standard Reference Seawater and within the temperature and salinity ranges of this study.

Suggested Reviewers: Lisa Miller Ph.D.
Fisheries and Oceans Canada, Pacific Region
Lisa.Miller@dfo-mpo.gc.ca
sea ice biogeochemistry & sea ice carbonate system expertise

Nicholas R. Bates Ph.D.
Bermuda Institute of Ocean Sciences, Bermuda
nick.bates@bios.edu
carbonate system - polar oceanic regions expertise

David Turner Ph.D.
University of Gothenburg, Göteborg, Sweden

david.turner@gu.se
carbonate system - seawater chemical models expertise

Bruno Delille Ph.D.
University of Liège, Liège, Belgium
Bruno.Delille@ulg.ac.be
sea ice biogeochemistry - carbonate system expertise

Simon Clegg Ph.D.
University of East Anglia, Norwich, UK
s.clegg@uea.ac.uk
expertise in seawater chemical models

Stathys Papadimitriou
Bangor University
College of Natural Sciences, Ocean Sciences
Askew Street, Menai Bridge
Anglesey LL59 5AB, UK
e-mail: s.papadimitriou@bangor.ac.uk

21 April 2017

FAO: Editor-in-Chief, Geochimica et Cosmochimica Acta

Dear Dr Norman,

I would like to submit to *Geochimica et Cosmochimica Acta* the attached manuscript titled "The stoichiometric dissociation constants of carbonic acid in seawater brines from 298 to 267 K" by S. Papadimitriou, S. Loucaides, V. M. C. Rérolle, P. Kennedy, E. P. Achterberg, A. G. Dickson, M. Mowlem, and H. Kennedy for consideration as a regular article. The manuscript describes work which is not published or under consideration for publication elsewhere. It presents the experimental determination of the dissociation constants of carbonic acid in natural seawater and seawater-derived brines to practical salinity 100 and from 25 °C to the freezing point of these solutions. To the best of our knowledge, the data set is new for salinities greater than 50 and, especially, at below-zero temperatures and has particular relevance to inorganic carbon investigations in polar oceanic environments. All authors have seen the manuscript and agree to its submission to the journal. We would like to suggest the following Associate Editors, who would be appropriate to handle the manuscript:

- Robert Byrne, University of South Florida, St. Petersburg, USA, e-mail: rhbyrne@usf.edu
- Jack Middelburg, Utrecht University, Utrecht, Netherlands, e-mail: J.B.M.Middelburg@uu.nl
- Alfonso Mucci, McGill University, Montreal, Canada, e-mail: alfonso.mucci@mcgill.ca

We also suggest the following reviewers:

- Lisa Miller, Fisheries and Oceans Canada, Pacific Region, e-mail: Lisa.Miller@dfo-mpo.gc.ca
- Nicholas R. Bates, Bermuda Institute of Ocean Sciences, Bermuda, e-mail: nick.bates@bios.edu
- David Turner, University of Gothenburg, Göteborg, Sweden, e-mail: david.turner@gu.se
- Bruno Delille, University of Liège, Liège, Belgium, e-mail: Bruno.Delille@ulg.ac.be
- Simon Clegg, University of East Anglia, Norwich, UK, e-mail: s.clegg@uea.ac.uk

Thank you.

Sincerely

Stathys Papadimitriou, Ph. D.

The stoichiometric dissociation constants of carbonic acid in seawater brines from 298 to 267 K

Stathys Papadimitriou[a,*], Socratis Loucaides[b], Victoire M. C. Rérolle[b,1], Paul Kennedy[a], Eric P. Achterberg[c,2], Andrew G. Dickson[d], Matthew Mowlem[b], Hilary Kennedy[a]

[a]Ocean Sciences, College of Natural Sciences, Bangor University, Menai Bridge, Anglesey LL59 5AB, UK

[b]National Oceanography Centre, Southampton, SO14 3ZH, UK

[c]University of Southampton, National Oceanography Centre, Southampton, SO14 3ZH, UK

[d]Marine Physical Laboratory, Scripps Institution of Oceanography, University of California, San Diego, 9500 Gilman Drive, La Jolla, CA 92093-0244, USA

[1]Present address: Sorbonne Universités (UPMC, Univ Paris 06)-CNRS-IRD-MNHN, LOCEAN Laboratory, 75005, Paris, France

[2]Present address: GEOMAR, Helmholtz Centre for Ocean Research, 24148 Kiel, Germany

[*]Corresponding author: s.papadimitriou@bangor.ac.uk (e-mail)

Abstract

The stoichiometric dissociation constants of carbonic acid (K_{1C}^* and K_{2C}^*) were determined by measurement of all four measurable parameters of the carbonate system (total alkalinity, total dissolved inorganic carbon, pH, and CO_2 fugacity) in natural seawater and seawater-derived brines, with a major ion composition equivalent to that of Standard Reference Seawater, to practical salinity (S_P) 100 and from 25 °C to the freezing point of these solutions and –6 °C temperature minimum. These values, reported in the total proton scale, provide the first such determinations at below-zero temperatures and for $S_P > 50$. The temperature (T, in Kelvin) and S_P dependence of the current pK_{1C}^* and pK_{2C}^* (as negative common logarithms) within the salinity and temperature ranges of this study ($33 \leq S_P \leq 100$, $-6\ °C \leq t \leq 25\ °C$) is described by the following best-fit equations: $pK_{1C}^* = -176.48 + 6.14528\,S_P^{0.5} - 0.127714\ S_P + 7.396\times10^{-5}S_P^2 + (9914.37 - 622.886\,S_P^{0.5} + 29.714\ S_P)\ T^{-1} + (26.05129 - 0.666812\,S_P^{0.5})\ \ln T$ ($\sigma = 0.011$, $n = 62$), and $pK_{2C}^* = -323.52692 + 27.557655\,S_P^{0.5} + 0.154922\ S_P - 2.48396\times10^{-4}S_P^2 + (14763.287 - 1014.819\,S_P^{0.5} - 14.35223\ S_P)\ T^{-1} + (50.385807 - 4.4630415\,S_P^{0.5})\ \ln T$ ($\sigma = 0.020$, $n = 62$). These functions are suitable for application to investigations of the carbonate system of internal sea ice brines with a conservative major ion composition relative to that of Standard Reference Seawater and within the temperature and salinity ranges of this study.

1. Introduction

The investigation of the carbonate system in aquatic environments is essential in the understanding and monitoring of the carbon cycle in the hydrosphere. Such investigations have intensified in the marine environment because of the crucial role the ocean plays in the absorption and storage of the anthropogenic CO_2 emitted to the atmosphere during the Industrial era (Takahashi et al., 1997; Sabine et al., 2004). Through this process, the ocean has become the main repository of anthropogenic CO_2 (Takahashi, 2004), with consequent chemical and ecosystem functioning effects from the acidification of surface oceanic waters (increased oceanic pH relative to pre-industrial era values) (Caldeira and Wickett, 2003; Feely et al., 2004; Takahashi et al., 2014; Gattuso et al., 2015). The acidification effect on the oceanic carbonate system by warming (Crowley, 2000) and atmospheric CO_2 absorption (Takahashi, 2004; Sabine et al., 2004) has been observed in surface coastal and pelagic waters (Takahashi et al., 2014), including large areas of the Arctic Ocean (Feely et al., 2008; Yamamoto-Kawai et al., 2009; Cai et al., 2010; Semiletov et al., 2016).

One of the challenges that remain in the high latitude (polar) oceans of the Earth's cryosphere is reliable determination of the carbonate system in the brine-ice system in the extensive seasonal sea ice cover of these environments (Brown et al., 2014; Miller et al., 2015; Papadimitriou et al., 2016). Early investigations in the composition and activity of the ice-associated (sympagic) microbial community in sea ice have uncovered the role of this multi-phase system on the surface of high latitude oceans as a habitat akin to other large-scale biomes, such as the desserts and tundra (Fritsen et al., 1994; Gleitz et al., 1995; Arrigo et al., 1997; Thomas and Dieckmann, 2002; Kennedy et al., 2002). Subsequent investigations have revealed a complex internal carbon cycle driven not only by the sympagic autotrophic and heterotrophic microbial communities, but also by two other major chemical reactions in the surface ocean, CO_2 gas exchange and hydrated $CaCO_3$ authigenesis (Papadimitriou et al., 2004; Delille et al., 2007; Dieckmann et al., 2008; Munro et al., 2010; Papadimitriou et al., 2012; Fischer et al., 2013). The internal carbon cycling in sea ice is complemented by measurable CO_2 fluxes to and from the atmosphere as a function of ice temperature (Delille et al., 2014) and to the underlying ocean by gravity drainage of the internal brines (Rysgaard et al., 2007; Rysgaard et al., 2011). These past investigations have culminated in a keen interest in the carbonate system of sea ice brines (Brown et al., 2014; Miller et al., 2015), the residual internal solution where all biogeochemical reactions occur either in

isolation from, or in direct exchange with, the adjacent seawater column and the atmosphere depending on the temperature- and salinity-dependent permeability of the medium (Golden et al., 1998). Sea ice brines are derived from the frozen surface seawater by physical concentration of the dissolved sea solutes following their expulsion from the ice crystal matrix. Along with degassed components, the brines can become trapped in pockets and channels in the sea ice structure. As a result of internal thermal equilibrium in sea ice along temperature gradients extending seasonally slightly above or far below the freezing point of seawater (–1.92 °C at 0 dbar pressure and salinity 35; Unesco, 1983), the salinity of internal brines can vary from the hyposaline to values in excess of 100 below –6 °C, and the concentration of brine solutes can likewise vary (Gleitz et al., 1995; Miller et al., 2011a, 2011b; Papadimitriou et al., 2012; Geilfus et al., 2012a).

The carbonate system in the marine environment is defined by pressure, temperature, salinity, the total concentration of boron and the dissociation constant of boric acid, the dissociation constants of carbonic acid, the value of two of its four measurable parameters [total alkalinity (A_T), total dissolved inorganic carbon (C_T), pH, and the fugacity of CO_2 (fCO_2)] and, lastly, the weak acid-base systems in the dissolved macro-nutrient and metabolite pools (phosphate, silicate, ammonium, sulphide) and their respective dissociation constants (Millero, 1995; Dickson et al., 2007). To date, all relevant dissociation constants have been adequately constrained empirically as a function of temperature and salinity for above-zero temperatures and practical salinity (S_P) up to 50 (Millero, 1995, and references there-in). Great investigative effort has been invested in the experimental determination of the first and second stoichiometric (concentration-based) dissociation constants of carbonic acid in seawater and solutions derived from seawater by dilution or evaporation, both in natural and artificial media with the mean stoichiometric composition of seawater (Hansson, 1973; Mehrbach et al., 1973; Goyet and Poisson, 1989; Roy et al., 1993; Mojica-Prieto and Millero, 2002; Millero et al., 2006). The determination of the carbonate system in the complex and sparsely accessible sea ice system is currently limited to direct measurements of A_T and C_T (Miller et al., 2015) and is further compounded by the large uncertainty in the values of the relevant acid-base dissociation constants as they are currently estimated via extrapolation of the existing different salinity-temperature functions to the physical sea ice conditions (temperature < 0 °C, S_P > 50) (Brown et al., 2014). Direct in-situ measurements of fCO_2 in the sea ice system are still rare either in bulk sea ice (Miller et al.,

2011a, b; Geilfus et al., 2012b) or in brines, which are, moreover, subject to the sparse spatial resolution afforded by brine collection in boreholes through the ice surface (Delille et al., 2007; Geilfus et al., 2012a; Delille et al., 2014). In addition, direct brine pH measurement has not been possible so far at below-zero temperatures and high salinities as a result of sampling and analytical difficulties in this complex system. As a first step towards the implementation of direct pH measurement in sea ice brines, the pH of Tris buffers (Papadimitriou et al., 2016) and the $p(K_2e_2)$ of the pH-indicator dye *meta*-Cresol Purple (Loucaides et al., 2017) have recently been characterized electrometrically with the Harned cell and spectrophotometrically, respectively, to $S_P = 100$ and –6 °C. Sea ice geochemists, therefore, have so far relied on indirect determination of brine fCO_2 and pH from the solution of the system of equations that describe the acid-base equilibria of the oceanic carbonate system using temperature, salinity, nutrient concentrations (if available), and the direct measurements of A_T and C_T as input parameters, with the caveats of extrapolation mentioned above (Brown et al., 2014).

Here, we present measurements that allowed the determination of the dissociation constants of carbonic acid in seawater and seawater-derived brines at below-zero temperatures to the freezing point of these solutions up to $S_P = 100$ and a temperature minimum of –6 °C. The S_P and temperature ranges of this study were set because the ionic composition and inter-ionic ratios in surface oceanic water are conserved in the natural sea ice brines over these temperature and salinity ranges. More concentrated, cooler sea ice brines ($S_P > 100$ and $t < –6$ °C) become supersaturated with respect to a suite of hydrated solid phases, including mirabilite, hydrohalite, and gypsum (Butler et al., 2016; Butler and Kennedy, 2015), thus altering the chemical composition and ionic ratios of the brines from those in surface oceanic water (Marion, 2001). Determination of equilibrium constants beyond the current salinity-temperature range must account for these compositional modifications (Hain et al., 2015) by solid-solution reactions, and so, it requires custom experimental protocols in a separate investigation.

2. Materials and Methods

The stoichiometric first (K^*_{1C}) and second (K^*_{2C}) dissociation constants of carbonic acid describe the equilibrium of the reactions, $CO_2^* + H_2O \leftrightarrow H^+ + HCO_3^-$ and $HCO_3^- \leftrightarrow H^+ + CO_3^{2-}$, respectively, with $[CO_2^*] = [CO_2(aq)] + [H_2CO_3]$ (Dickson et al., 2007). In this study, they were determined in natural high ionic strength solutions (seawater, seawater-derived brines) from

measurements of A_T, C_T, fCO_2, and $pH_T = -\log[H^+]_T$ (total proton scale) as follows (Millero et al., 2002):

$$K^*_{1C} = [H^+]_T \frac{2C_T - A_C - 2[CO^*_2]}{[CO^*_2]}, \quad (1)$$

$$K^*_{2C} = [H^+]_T \frac{A_C - C_T + [CO^*_2]}{2C_T - A_C - 2[CO^*_2]}, \quad (2)$$

In the above equations, A_C = carbonate alkalinity = $[HCO_3^-] + 2[CO_3^{2-}]$, $C_T = [CO^*_2] + [HCO_3^-] + [CO_3^{2-}]$, and $[CO^*_2] = K_o\, fCO_2$, with K_o = CO_2 solubility constant as a function of salinity and temperature (Weiss, 1974), and brackets denoting total concentrations (single ion plus ion pairs in the case of pair-forming ionic species). Carbonate alkalinity was determined from the measured A_T and pH_T as described in Millero et al. (2002). To this end, the contributions of dissolved phosphate and silicic acid to A_T were computed from their measured total concentrations, the measured pH_T, and the relevant stoichiometric equilibrium dissociation constants computed from the available salinity-temperature functions (Millero, 1995; Dickson et al., 2007). For the contribution of total boron (B_T) to A_T, the mean B_T concentration in S_P = 35 seawater as computed from the data in Lee et al. (2010), $[B_T]$ = 0.000432578 mol $kg^{-1}_{solution}$ (hereafter, mol kg^{-1}), was used as a linear function of salinity (Millero, 1995), along with the measured pH_T and the stoichiometric equilibrium dissociation constant of boric acid in Dickson (1990). The contributions of OH^- and protons (concentration on the seawater scale: $[H^+]_{SWS} = [H^+] + [HSO_4^-] + [HF]$) to A_T were determined using the measured pH_T and the relevant equilibrium constants from the available oceanographic functions (Millero, 1995; Dickson et al., 2007) along with the concentrations of SO_4^{2-} and F^- in Standard Reference Seawater as a linear function of salinity (Millero et al., 2008). The oceanographic functions for the equilibrium constants used for these computations were extrapolated outside their empirical salinity-temperature ranges when the experimental conditions extended beyond them. Locally sourced seawater (Menai Strait; 53.1806N 4.2333W), UV-sterilized and filtered through a 0.2 μm filter, was used as the experimental medium (S_P = 33 – 34) and for the preparation of the experimental brines (S_P = 40 – 100) by variable freezing and gravimetric dilution, when needed, with Milli-Q

water. The brines were filtered through pre-combusted (500 °C, 3 hrs) GF/F filters (0.7 μm, WHATMAN); they were then sampled for the determination of major ion concentrations (Na^+, K^+, Ca^{2+}, Mg^{2+}, Cl^-, SO_4^{2-}) and were kept stored at room temperature in the dark in acid-washed glass media bottles (DURAN) capped (gas-tight) with Teflon-lined screw-caps.

The experiments were conducted at zero and below-zero temperatures to very near the freezing point of seawater and seawater-derived brines, as well as at above-zero temperatures to 25 °C, in order for our experimental results to span the existing data sets for the stoichiometric dissociation constants of carbonic acid in natural seawater and brines for validation. The freezing point of the experimental brines was calculated from the empirical absolute salinity-temperature relationship of thermally equilibrated sea ice brines, $S_A = 1000\ [1 - (54.11/t)]^{-1}$ (Assur, 1958), with S_A (in g kg^{-1}) and conductivity-based salinity (S_P) related by $S_A = 1.004715 S_P$ (Millero and Huang, 2009).

Each salinity-temperature experiment was conducted with ~1.1 L seawater or brine in a Teflon-lined-capped media bottle (DURAN), which was thermally equilibrated by immersion in a thermostated ethylene-glycol/water bath (GRANT TX150) and was kept at constant temperature during measurement and sampling for the analysis of the required parameters. The experimental temperature was monitored with a Fluke 5609 Platinum Resistance Probe on a Hart Scientific 1502A Thermometer and is reported as the mean of the values recorded for the duration of each experiment. Throughout the experiment, the sample was gently stirred (50 rpm) with an overhead stainless steel stirrer through the cap. Each experiment required about 70 minutes to complete the necessary measurements (fCO_2 and pH_T) at the experimental temperature and the sample collection for the remainder of analyses. First, the fCO_2 and pH_T measurements were conducted simultaneously in separate aliquots of the sample, drawn through Tygon® tubings with a Watson Marlow 520U peristaltic pump towards the CO_2 Analyzer unit and the pH unit. Upon completion of these measurements, samples for C_T determination were pump-drawn and flame-sealed into pre-weighed 10 mL glass ampoules poisoned with saturated mercuric chloride. Subsequently, samples for soluble reactive phosphorus (SRP, hereafter, phosphate) and molybdenum reactive silicon [hereafter, silicic acid, $Si(OH)_4$] were removed and the remaining sample was used for replicate A_T determinations.

2.1 fCO_2 measurement

192 The fCO_2 was determined from the CO_2 mole fraction (x_{CO_2}) measured on a LICOR 840A
193 CO_2/H_2O analyzer of the dry gas generated in a closed loop by exchange with the sample via a
194 0.5×1 MicroModule™ Membrane Contactor (Liqui-Cell; www.liquicell.com), used here as the
195 gas exchange unit (Hales et al., 2004a). The gas was circulated in the closed loop at 48 mL min^{-1}
196 through a custom-made DRIERITE desiccant column (www.drierite.com) with a custom-made
197 gas micro-pump. The contactor was immersed in a custom-made housing in the same water bath
198 as the sample, which was pumped through the contactor at 9 mL min^{-1} in Tygon® tubing via the
199 Watson Marlow 520U peristaltic pump. The temperature of the sample in the bottle and at the
200 exit of the contactor was monitored with type K thermocouple probes by continuous logging on a
201 Pico Technology USB TC-08 thermocouple data logger. In this set-up, a plateau in x_{CO_2} was
202 achieved in 50 min, and the x_{CO_2} used for fCO_2 determination in each thermostated sample was a
203 5 min average of recorded values within the plateau phase. These values were within 1 ppm for
204 x_{CO_2} < 1000 ppm and within 3 ppm for x_{CO_2} > 1000 ppm. The measurements were calibrated
205 against CO_2/N_2 mixtures with a certified x_{CO_2} (0, 20, 100, 400, 1000, and 2000 ppm; uncertainty
206 ≤ 5%, BOC, boc.com). The calibrations were conducted between two consecutive experiments.
207 The sample fCO_2 was computed from the measured x_{CO_2} as in SOP 5 in Dickson et al. (2007),
208 using the pressure readings from the built-in barometer in the LICOR gas cell.

209 An estimate of the uncertainty of these measurements was possible at above-zero
210 temperatures by analyzing, with this protocol, samples of CO_2 in Seawater Certified Reference
211 Materials (CRM, Batches #112, #124, and #125; Scripps Institution of Oceanography) and
212 comparing the measured fCO_2 with that computed from the certified C_T and A_T, as well as the
213 salinity and the phosphate and silicic acid concentrations reported in the certificate. The CRM
214 fCO_2 analyses were thus conducted every 1 – 4 °C in the temperature range from 3.16 °C to 24.99
215 °C (batch #112: n = 11; batch #124, n = 1; batch #125, n = 1). For the calculations, the first and
216 second dissociation constants of carbonic acid were computed from the salinity-temperature
217 functions based on the measurements of Mehrbach et al. (1973) as refitted on the total proton
218 scale by Lueker et al. (2000). The dissociation constants of the remainder of the weak acids and
219 bases of the oceanic carbonate system, the solubility of CO_2 in seawater, and the B_T and the total
220 dissolved sulphate and fluoride concentrations were computed as described earlier. All
221 computations were conducted on the total proton scale by solving for pH the system of equations

that describe the equilibria of the marine carbonate system using the Solver routine on Microsoft Excel. At the computed CRM fCO_2 from 225 µatm at 3.16 °C to 567 µatm at 24.99 °C for batch #112 and 537 µatm at 22.03°C for batch #124, the measured fCO_2 differed by –9 ± 10 µatm (n = 12), while the measured fCO_2 differed by –85 µatm at CRM fCO_2 = 1062 µatm at 18.06 °C for batch #125, suggesting the potential for a negative bias at high fCO_2.

2.2 pH measurement

The pH_T (total proton scale) was determined spectrophotometrically using purified *meta*-Cresol Purple (mCP) indicator dye (Liu et al., 2011) and the custom-made micro-opto-fluidic Lab-On-Chip (LOC) pH system described in Rérolle et al. (2013). The LOC unit with its sample and dye inlets, as well as the optics (photodiode detector and light source) were all custom-housed and immersed as a separate micro-unit in the same thermostated water bath as the sample and the fCO_2 contactor described in the previous section. The electronics, pumps, and reagent stores were outside the water bath. The mCP used in this study was purified and was characterized for the variation of its optical parameters and second dissociation constant (on the total proton scale) in the salinity and temperature conditions of this investigation as reported in Loucaides et al. (2017). The pH_T is reported as the mean of several injections (5 – 10) per sample through the LOC pH system. In the case of the pH_T measurements used in the determination of K_{1C}^* and K_{2C}^* (eqs. 1 and 2), these multiple injections occurred over the course of the simultaneous fCO_2 determination, with a reproducibility better than 0.004 pH unit (as 1σ). The accuracy of the pH_T measurement protocol was assessed against the pH_T computed for CRMs as described in the previous section. The CRM pH analyses were thus conducted every 1 – 2 °C in the temperature range from 1.52 °C to 25.15 °C using CRM batches #112 (n = 5), #124 (n = 1), and #125 (n = 1), which were also used for the fCO_2 protocol validation described in the previous section, as well as batch #138 (n = 15), used here only for the validation of the pH measurement protocol. At the computed CRM pH_T for batches #112 (7.908 at 24.99 °C to 8.264 at 1.97 °C), #124 (7.927 at 22.03 °C), and #138 (7.852 at 25.15 °C to 8.215 at 1.52 °C), the measured pH_T differed by –0.013 ± 0.011 (n = 21) pH unit. For the high-fCO_2 CRM batch #125 (CRM pH_T = 7.659 at 18.06 °C), the measured pH_T differed by +0.015 pH unit.

2.3 A_T and C_T measurements

253 Total alkalinity was determined by potentiometric titration with 0.1 N HCl at 20 °C using the
254 Gran function for pH < 3.5 (Gleitz et al., 1995; Papadimitriou et al., 2013) with a Metrohm
255 Titrando 888 unit of automatic burette, pH meter, Pt temperature probe, Ag/AgCl/KCl reference
256 electrode, and glass indicator electrode calibrated with buffers traceable to SRM from NIST and
257 PTB (Merck, pH 2.00, 4.01, 7.00, 9.00, and 10.00 at 25 °C). The titration was conducted in
258 replicate ~100 mL aliquots of known weight at constant pCO_2 (400 ppm CO_2) provided at a
259 controlled rate (200 mL min^{-1}) via a CHELL CMD100 microprocessor controller and Hastings
260 Mass Flow Control Valve. The rigour of the technique was assessed from several titrations of
261 CRM batch #112 (A_T = 2223.26 μmol kg^{-1}) with a coulometry-characterized HCl solution
262 (0.100171 mol HCl kg^{-1}, ~0.7 M NaCl; Scripps Institution of Oceanography), yielding a
263 difference of measured from certified A_T of –1.9 ± 1.7 μmol kg^{-1} (n = 23), equivalent to 0.08%
264 reproducibility and accuracy. Batches of 0.1 N HCl were also prepared gravimetrically in the
265 course of this study to a total ionic strength of 0.72 molal using NaCl, and the HCl concentration
266 was calibrated against the A_T of CRM batches #112 and #138. The difference between the A_T
267 measured with these acid batches and the certified concentrations was –1.1 ± 2.8 μmol kg^{-1} (n =
268 99) in good agreement with that determined with the Scripps CRM and acid. Because the acid
269 batches were calibrated against seawater CRMs and the response of commercial glass electrodes
270 may be unreliable in hypersaline solutions, the A_T in brines was determined in samples diluted to
271 a salinity of 34 with Milli-Q water. The A_T of the brine batches (Table 2), normalized to salinity
272 35, was $A_{T,35}$ = 2424 ± 39 μmol kg^{-1} (n = 10), while the local seawater had a two-year (2014-
273 2015) average $A_{T,35}$ = 2398 ± 22 μmol kg^{-1} (n = 37).
274 The C_T concentration was determined manometrically in 3 – 10 replicate sample aliquots
275 (~10 mL) from the CO_2 generated and extracted in vacuo in a glass manifold following reaction
276 of a weighed sample aliquot with H_3PO_4 and cryogenic CO_2 gas distillation in successive cold (–
277 95 ºC) methanol and liquid nitrogen traps, using an in-line manometer (CHELL) and a virial
278 equation of state (Bockmon and Dickson, 2015). The reproducibility of these measurements was
279 better than 0.4% in the 2000 to 5600 μmol kg^{-1} concentration range. Determination of C_T on
280 CRM batches #112, #124, #125, and #138 (Scripps Institution of Oceanography) yielded a
281 difference between the measured and certified C_T as an accuracy (± reproducibility as 1σ) of +0.7
282 ± 8.8 μmol kg^{-1} (n = 111).
283

284 **2.4 Other measurements**

285 The salinity of the experimental solutions was measured at laboratory temperature (~20 ºC)
286 using a portable conductivity meter (WTW Cond 3110) with a WTW Tetracon 325 probe. When
287 salinities exceeded 70, they were determined following gravimetric dilution with distilled water.
288 The initial major ion composition of the brines was determined as follows: (*i*) potentiometric
289 titration with EDTA as titrant and Tris-buffered acetylacetone (0.1 M) as the complexing agent at
290 pH ~8.5 for Ca^{2+} and Mg^{2+} as described in Papadimitriou et al. (2012), (*ii*) ion chromatography
291 on a Dionex Ion Exchange Chromatograph ICS 2100 for Na^+ and K^+, (*iii*) gravimetric Mohr
292 titration for Cl^- with 0.3 mol kg^{-1} $AgNO_3$ standardized against NaCl purified by re-crystallization
293 (Dickson, 1990; Millero et al., 1993), and (iv) for SO_4^{2-}, precipitation as $BaSO_4$ in EDTA
294 followed by titration with $MgCl_2$ (Howarth, 1978). The phosphate and silicic acid concentrations
295 were determined within 4 to 8 weeks from collection on refrigerated aliquots stored in acid-
296 washed (2 N HCl) 20 mL PE vials. These analyses were conducted on a SEAL AA3 MR
297 continuous segmented flow autoanalyzer using standard colorimetric methodology (Hales et al.,
298 2004b).
299
300 **2.5 Error analysis**

301 The error in the experimental K_{1C}^* and K_{2C}^* values was computed as $\sigma^2_{K_{iC}^*} = \sum[(dK_{iC}^*/dX)\,\sigma_X]^2$
302 (Barford 1985), with X = H^+, C_T, A_C, CO_2(aq) (all in mol kg^{-1}). The maximum measurement
303 uncertainty (σ_X) was 0.020 pH unit for the pH measurements, 0.4% for the C_T determinations, 20
304 µatm for fCO_2 < 1000 µatm, 90 µatm for fCO_2 > 1000 µatm, and 0.1% for the A_C estimates based
305 on the uncertainty of the A_T measurement. The magnitude of the extrapolation error for the
306 estimates of the individual A_T components is unknown at this stage. The available measurement
307 uncertainties in pH_T, C_T, fCO_2, and A_C determinations indicated that K_{1C}^* is most sensitive to
308 uncertainties in the pH and fCO_2 measurements, while K_{2C}^* is most sensitive to the uncertainties
309 in the A_C estimates and the C_T and pH measurements. The K_{1C}^* uncertainty was thus calculated to
310 range from 0.020 – 0.040 pK unit at fCO_2 > 250 µatm to 0.050 pK unit at fCO_2 < 250 µatm. The
311 K_{2C}^* uncertainty was calculated to be 0.040 pK unit for our experiments. The uncertainties of
312 both constants in this study are therefore estimated to be about twice those reported for standard

oceanographic conditions (0.020 pK unit for K_{1C}^* and 0.030 pK unit for K_{2C}^*; Dickson and Millero, 1987).

2.6 Data evaluation

The K_{1C}^* and K_{2C}^* determinations in seawater at above-zero temperatures were evaluated against the existing major data sets in natural seawater, i.e., the Mehrbach et al. (1973) data set (experimental ranges: S_P = 19 – 43, t = 2 – 35 °C) as refitted on the total proton scale by Lueker et al. (2000) and the Millero et al. (2006) data set (experimental ranges: S_P = 1 – 51, t = 1.0 – 50.5 °C). Because the latter data set has been reported on the seawater proton scale, it was converted to the total proton scale as described in Millero (1995) and was re-fitted here using the same equation format as in the original study:

$$pK_{iC}^* = pK_{iC}^o + A_i + B_i/T + C_i \ln T \ (i = 1, 2), \qquad (3)$$

In the above equation, T = temperature (in Kelvin), $A_i = a_o S_P^{0.5} + a_1 S_P + a_2 S_P^2$, $B_i = a_3 S_P^{0.5} + a_4 S$, $C_i = a_5 S_P^{0.5}$, and $pK_{iC}^o = b_o + b_1/T + b_2 \ln T$ = thermodynamic dissociation constant, with a_o, a_1, a_2, a_3, a_4, a_5 = best-fit parameters (Table 3) determined by non-linear regression using the Excel regression routine, while b_o, b_1, and b_3 are from Millero et al. (2006). The standard error of the fit was the same as in the original study ($\sigma_{pK_{1C}^*}$ = 0.006 and $\sigma_{pK_{2C}^*}$ = 0.011).

The current pK_{1C}^* and pK_{2C}^* determinations in natural seawater (S_P = 33 – 34; mean S_P = 33.66 ± 0.36, n = 5) over the temperature range from 0 to 25 °C (Table 2) are in very good agreement with the previously published data sets (Fig. 1). Specifically, in the 0 – 25 °C temperature range, the current observations (n = 23) differed by ΔpK_{1C}^* = –0.009 ± 0.016 and ΔpK_{2C}^* = +0.002 ± 0.018 relative to the Mehrbach et al. (1973) data set, and ΔpK_{1C}^* = –0.014 ± 0.017 and ΔpK_{2C}^* = –0.003 ± 0.022 relative to the Millero et al. (2006) data set, all within experimental error. The determinations beyond the salinity-temperature bounds of the available oceanographic data sets (t < 0 °C, S_P > 50) were compared with the extrapolated values of the oceanographic equations as will be discussed in the *sections 3* and *4*. In addition, the K_{1C}^* and

K^*_{2C} determinations near the freezing point of seawater and seawater-derived brines from this study were compared with the values calculated from appropriate thermodynamic data as follows. Stoichiometric equilibrium constants are related to the thermodynamic constants at infinite dilution (pure water) via the activity coefficients of the reacting ions. In the case of K^*_{1C} and K^*_{2C}, this relationship is given by the following equations (Millero et al., 2006):

$$K^*_{1C} = K^o_{1C} \frac{\gamma_{CO_2} \alpha_{H_2O}}{\gamma_{H^+} \gamma_{HCO_3^-}} \Theta, \quad (4)$$

$$K^*_{2C} = K^o_{2C} \frac{\gamma_{HCO_3^-}}{\gamma_{H^+} \gamma_{CO_3^{2-}}} \Theta, \quad (5)$$

where K^o_{1C}, K^o_{2C} = thermodynamic dissociation constants of carbonic acid, α_{H_2O} = activity of water, γ_i = total ion activity coefficient (i = CO_2(aq), H^+, HCO_3^-, CO_3^{2-}) (in mol $kg^{-1}_{H_2O}$), and Θ = 1 – 0.001005 S_P = conversion factor from mol $kg^{-1}_{H_2O}$ to mol $kg^{-1}_{solution}$ (Millero, 1995). For the calculation of the required thermodynamic dissociation constants, α_{H_2O}, and γ_i at below-zero temperatures, the database of the FREZCHEM code (version 15.1) was used here, which is the most frequently used to examine geochemical processes in the cryosphere and is based on the Pitzer formalism of ionic interactions in strong electrolyte solutions (Marion, 2001; Marion et al., 2010). The FREZCHEM v15.1 includes some of the equilibria of the aqueous carbonate system (boron and fluoride chemistry, $CaCO_3$-solution equilibrium) and is rooted in the extant above-zero temperature data of the relevant thermodynamic equilibrium constants and Pitzer coefficients, with additional validation at below-zero temperatures from the metal-carbonate solubility data of the early 20th century Russian literature mostly at the eutectic point of these salt solutions (Marion, 2001). The model was run in the freezing mode (ice-water equilibrium) at 0.1 °C steps from 0 to –6 °C at 1 atm and a fixed pCO_2 at 400 μatm (non-conservative C_T) for a starting ionic composition equivalent to the reference composition for seawater of salinity 35 (Millero et al., 2008), with all other solid phases disabled (conservative major ionic composition and A_T). Total ion activity coefficients are directly proportional to the free ion activity coefficients, with the concentration ratio of the free ion to the sum of the free ion and ion pairs as

the proportionality factor (Pytkowicz and Kester, 1969). In the case of the total proton scale used in this study, $\gamma_{H^+} = \gamma_{H^+,free}\ m_{H^+,free} / (m_{H^+,free} + m_{HSO_4^-})$ (Millero, 1995), with m = molality (in mol $kg^{-1}_{H_2O}$) and all quantities in the right side of this equation obtained from the output of the code. The FREZCHEM code computes α_{H_2O}, γ_{CO_2}, and the single ion activity coefficients of HCO_3^- and CO_3^{2-} from the Pitzer equations (Pitzer, 1973) and relevant Pitzer parameters. All ion pairs for HCO_3^- are considered adequately represented in the Pitzer computation (He and Morse, 1993) and so, the single ion activity coefficient of HCO_3^- in the code output is equivalent to $\gamma_{HCO_3^-}$ in eqs. (3) and (4). The code takes into account explicitly ion pair formation for CO_3^{2-} in the form of $CaCO_3^o$ and $MgCO_3^o$ (He and Morse, 1993; Marion, 2001). The molalities of these ion pairs were taken into account along with the molality and activity coefficient of CO_3^{2-} as a single ion in the code output to compute the total activity coefficient of CO_3^{2-} ($\gamma_{CO_3^{2-}}$) for use in eqs. (3) and (4) by applying the same principle as outlined above for γ_{H^+}.

2.7 Application to sea ice brines

A simple numerical model was used to illustrate the changes in the parameters of the carbonate system in seawater-derived brines with (*i*) conservative major ionic composition, A_T, and C_T, and (*ii*) brines of otherwise conservative chemical composition but at constant fCO_2 and, hence, non-conservative C_T, such as that which will occur as a result of dissolved-gaseous CO_2 exchange to atmospheric equilibrium. These scenarios are chosen for their simplicity for illustration purposes and cannot reflect the complexity of the carbonate system in sea ice brines as it is driven by several internal brine reactions at different and varying rates (Papadimitriou et al., 2004; Papadimitriou et al., 2007; Delille et al., 2007; Dieckmann et al., 2008; Munro et al., 2010; Geilfus et al., 2012a; Papadimitriou et al., 2012; Delille et al., 2014). The model was described in detail in Papadimitriou et al. (2014); briefly, it uses as a system of equations the weak acid-base equilibria in seawater, the salinity-normalized measured concentrations of phosphate, $Si(OH)_4$, C_T, and A_T in surface waters of the seasonal sea ice zone (SIZ) in the western Weddell Sea, Antarctica, reported in Papadimitriou et al. (2012), along with the concentrations of SO_4^{2-} and F^- in reference seawater (Millero et al., 2008) and the mean total

boron concentration in oceanic waters from Lee et al. (2010). In scenario (*i*) above, all these concentrations are conserved as a linear function of salinity, and the set of equations is solved for pH_T from A_T and C_T at each salinity-temperature pair at the freezing point of brines, allowing computation of the C_T speciation. In scenario (*ii*) above, all concentrations are conserved except C_T, and the system is solved for pH_T from fCO_2 and A_T, yielding C_T and its speciation. In this case, the fCO_2 was set at a constant value computed for 1 atm total pressure as described in Pierrot et al. (2009) from the average 2015 atmospheric CO_2 molar ratio (www.esrl.noaa.gov/gmd/ccgg/trends/). These calculations were done using the K^*_{1C} and K^*_{2C} determined in this study, as well as the values computed by extrapolation beyond their salinity maximum and temperature minimum of the salinity-temperature oceanographic functions described in the previous section.

3. Results

The initial composition of the brines for all major ions (Table 1), normalized to salinity 35, was in very good agreement with that of reference seawater (Millero et al. (2008) except for K^+, which was less by 1 mmol kg^{-1} on average, likely as a result of shading of the K^+ peak by the much greater Na^+ peak during ion chromatographic analysis. The conservative composition of the brines relative to that of reference seawater indicates no measurable alteration due to production of authigenic $CaCO_3$, $CaSO_4$, or Na_2SO_4 polymorphs over the short time scales of variable freezing of the seawater (6 – 15 hours) used here for brine preparation. It also justifies the use of the ionic composition of reference seawater in the thermodynamic evaluation of the current determinations of the stoichiometric dissociation constants of carbonic acid.

The measured parameters and the determined stoichiometric dissociation constants of carbonic acid (as negative common logarithms, pK^*_{1C} and pK^*_{2C}) are given in Table 2, with pK^*_{1C} and pK^*_{2C} reported in the total proton scale of the pH measurements. In the narrow below-zero temperature range to the freezing point of seawater (Table 2; t_{FP} = –1.82°C for batch S_P = 33.14; Unesco, 1983), the current observations (n = 6) were systematically higher than, but within experimental error from, the values determined by below-zero temperature extrapolation of the best-fit curves on the existing data sets, with an overall ΔpK^*_{1C} = +0.015 ± 0.005 and ΔpK^*_{2C} = +0.019 ± 0.015 relative to both the Mehrbach et al. (1973) and Millero et al. (2006) data sets

(Fig. 1). The measurements from natural brines (Table 2) from S_P = 40 to S_P = 100 and from 25 °C to near their freezing point (from –2.1 °C at S_P = 40 to –6.0 °C at S_P = 100) demonstrate that the determined pK^*_{1C} and pK^*_{2C} at S_P > 60 differ substantially at all temperatures from the values derived from the extrapolation of the existing oceanographic salinity-temperature functions (Fig. 2). Specifically, the current values are between the extrapolated values derived from the two oceanographic data sets used here for comparison. The greatest differences between measured and extrapolated values were seen at the highest salinities in the pK^*_{2C} relative to the best-fit equation derived from the Millero et al. (2006) data set, with ΔpK^*_{2C} = +0.72 ± 0.09 (n = 5) and +1.26 ± 0.12 (n = 6) at S_P = 85 and S_P = 100, respectively. For comparison, the equivalent ΔpK^*_{1C} was +0.13 ± 0.04 and +0.24 ± 0.07 at S_P = 85 and S_P = 100, respectively. The difference between the current and extrapolated values derived from the best fits to the Mehrbach et al. (1973) data set were similar for both pK^*_{1C} and pK^*_{2C} at the highest salinities (Fig. 2) and were more modest than those from the extrapolation of the Millero et al. (2006) data set, with ΔpK^*_{1C} = –0.19 ± 0.02 and ΔpK^*_{2C} = –0.12 ± 0.02 (n = 5) at S_P = 85 and ΔpK^*_{1C} = –0.32 ± 0.05, ΔpK^*_{2C} = –0.21 ± 0.04 (n = 6) at S_P = 100.

4. Discussion

4.1. The stoichiometric dissociation constants of carbonic acid

It is of note that pK^*_{2C} changed more dramatically (over 0.40 pK unit) than pK^*_{1C} (over 0.05 pK unit) as a function of salinity at all temperatures in the current experiments (Fig. 2). This suggests an equally strong difference in the change in the total activity coefficients of the bicarbonate and carbonate ions in increasingly more concentrated multi-electrolyte solutions. This is corroborated by the output of the FREZCHEM thermodynamic code at the freezing point of conservative seawater and seawater-derived brines, which yielded a monotonic decrease by a factor of 1.2 in $\gamma_{HCO_3^-}$ from 0.5780 at –1.9 °C to 0.4733 at –6.0°C and by a factor of 2.9 in $\gamma_{CO_3^{2-}}$ from 0.0550 at –1.9 °C to 0.0192 at –6.0°C.

The pK^*_{1C} computed from the output of the FREZCHEM thermodynamic code for the composition of multi-electrolyte solutions at ice-water equilibrium was in excellent agreement with the current freezing point observations (Fig. 3). According to eq. (4), this indicates that all

relevant thermodynamic parameters (K^{o}_{1C}, γ_{CO_2}, $\gamma_{HCO_3^-}$, γ_{H^+} and α_{H_2O}) are predicted reliably by the FREZCHEM code in the temperature range from the freezing point of seawater to that of S_P = 100 seawater-derived brine: K^{o}_{1C}, γ_{CO_2}, and $\gamma_{HCO_3^-}$ via extrapolation of the relevant above-zero temperature data sets of He and Morse (1993) and Plummer and Busenberg (1982), γ_{H^+} from the Pitzer parameters for the specific interaction of the proton with all other ions in the model solutions, and α_{H_2O} from the Pitzer parameterization of the osmotic coefficient. This was not the case, however, for pK^{*}_{2C}, with differences up to 0.2 pK unit between current determinations and FREZCHEM-derived values (Fig. 3), which is higher than experimental uncertainty. A similar discrepancy trend was observed in the study of the stoichiometric equilibrium solubility product of ikaite in Papadimitriou et al. (2013). Based on eqs. (4) and (5), the disagreement in pK^{*}_{2C} with the thermodynamic code suggests uncertainty in K^{o}_{2C} or the total activity coefficient of CO_3^{2-}, or both, at below-zero temperatures. The total activity coefficient of CO_3^{2-} depends strongly on the extent of ion pair formation in solution. Its ion pairs with Ca^{2+} and Mg^{2+} have high equilibrium association constants which have to be taken into account explicitly in Pitzer parameterization routines, such as FREZCHEM, to complement the formal Pitzer parameterization of the CO_3^{2-} interactions in multi-electrolyte solutions (He and Morse, 1993; Marion, 2001). Knowledge about the behaviour of these strong ion pairs is based on the above-zero temperature study of Plummer and Busenberg (1982), while the Pitzer parameters for the single ion activity coefficient of CO_3^{2-} are based on the above-zero temperature experiments of He and Morse (1993). It is conceivable that targeted relevant experiments that will expand the empirical thermodynamic data base for the C_T species to below-zero temperatures may reconcile such differences as that seen here with respect to CO_3^{2-} (Fig. 3). This is in line with the objectives of the recent SCOR Working Group 145 for the update of chemical speciation modelling in seawater (Turner et al., 2016).

The pK^{*}_{1C} and pK^{*}_{2C} values determined in this study were fitted to the same equation format (eq. 3) as described in *Section 2.6*, and the best-fit coefficients are given in Table 3. The standard error of the fit was $\sigma_{pK^{*}_{1C}}$ = 0.011 and $\sigma_{pK^{*}_{2C}}$ = 0.020, and the fitted residuals demonstrated no significant trends as a function of salinity and temperature (Fig. 4). These equations are suitable for interpolation within the salinity and temperature ranges of this investigation ($33 \leq S_P \leq 100$, –

483 6 °C ≤ t ≤ 25 °C) in conservative seawater-derived brines. They are not recommended for
484 extrapolation in the hyposaline and more hypersaline regions of the salinity spectrum, not least
485 because, at the coldest part of sea ice temperature (t < –6 °C) where S_P > 100, the brine inclusions
486 will have non-conservative ionic composition and altered major ionic ratios as a result of
487 reactions with authigenic ikaite, mirabilite, gypsum, and hydrohalite (Papadimitriou et al., 2013;
488 Butler and Kennedy, 2015; Butler et al., 2016). This will affect the value of stoichiometric
489 equilibrium constants (Hain et al., 2015), which must be determined in the context of authigenic
490 mineral-brine equilibria.
491
492 **4.2. The carbonate system in sea ice**
493 The simple numerical model described in *Section 2.7* was used to compute the change in pH_T,
494 fCO_2, and CO_3^{2-} with decreasing temperature from the freezing point of S = 35 seawater to –6 °C
495 in sea ice brines (Fig. 5). In brines which are conservative with respect to major ionic
496 composition, A_T, and C_T, the pK_{1C}^* and pK_{2C}^* equations derived in this study predict a monotonic
497 decrease in the pH_T from 8.028 to 7.862 coupled with increase in both the internal brine fCO_2
498 from 429 to 2225 μatm and the CO_3^{2-} concentration from 84 to 326 μmol kg^{-1}. These changes are
499 anticipated solely from the physical concentration of the weak acids and bases during the
500 expulsion of seawater solutes from the ice crystal matrix in the process of sea ice formation and
501 further cooling to –6 °C. If gas exchange occurs during seawater freezing and cooling of the sea
502 ice system with all major ions and A_T conserved in the internal brines, the composition of the
503 brines is non-conservative with respect to C_T and, as a result, the brine fCO_2 is controlled by its
504 equilibrium solubility. In this case, if atmospheric equilibrium is achieved in the brines, the brine
505 pH_T is predicted to increase from 8.059 to 8.479 and the CO_3^{2-} concentration will also increase
506 but to a much larger extent from 89 to 998 μmol kg^{-1}.
507 The advantage gained by the current K_{1C}^* and K_{2C}^* data set relative to the extrapolation of the
508 oceanographic equations parameterized for above-zero temperatures and S_P < 50 is evident in the
509 difference in absolute values for all parameters concerned here. Of the two major oceanographic
510 data sets used here for comparison, the extrapolation of the equations based on the Mehrbach et
511 al. (1973) data set yielded the smallest such differences (Fig. 5), especially with respect to CO_3^{2-}
512 in the conservative brine scenario (mean difference: –0.1 ± 4.3 μmol kg^{-1}) (Fig. 5c), for which the

513 mean brine pH_T = 7.92 ± 0.06 over the temperature range of the simulation. At the temperature
514 minimum of this study and depending on the set of extrapolated oceanographic pK^*_{1C} and pK^*_{2C}
515 equations, these differences were calculated to be up to +0.9 pH unit and –6000 μatm fCO_2 in the
516 conservative brine C_T scenario (Figs. 5a-c), as well as up to –1300 μmol CO_3^{2-} kg^{-1} in the non-
517 conservative brine C_T scenario (Fig. 5f). Similar differences have been reported as perplexing
518 uncertainties of extrapolation in the sensitivity analysis for the sea ice brine carbonate system
519 within S_P = 50 – 70 in Brown et al. (2014). It highlights the importance of re-evaluating the
520 coefficients of the existing salinity-temperature functions on empirical data when applied to
521 extended conditions.

522 Direct measurements at below-zero temperatures are rare for fCO_2 in sea ice brines (Delille et
523 al., 2007; Geilfus et al., 2012a; Delille et al., 2014) or bulk sea ice (Miller et al., 2011a, b; Geilfus
524 et al., 2012b) and have not been possible until recently for pH (Loucaides et al., 2017) due to
525 sampling and analytical difficulties in this complex medium. Sea ice geochemists thus far have
526 often relied on indirect determination of brine fCO_2 and pH in sea ice from direct measurements
527 of A_T and C_T to determine the brine carbonate system, with the caveats of extrapolation (Brown
528 et al., 2014), in order to assess the inorganic carbon budget in sea ice (Papadimitriou et al., 2007;
529 Delille et al., 2007; Munro et al., 2010; Fransson et al., 2011; Geilfus et al., 2012a; Papadimitriou
530 et al., 2012). The results of this study will provide confidence in the output of indirect parameter
531 determination for the carbonate system in the below-zero temperature range in high salinity
532 brines in parts of sea ice that are still warm enough to allow exchange with the air and the ocean.
533 Additional studies are still required to extend the current empirical data base of the dissociation
534 constants of carbonic acid to the coldest temperature spectrum of sea ice to the eutectic and, also,
535 to determine the behavior of the remainder weak acids and bases of the carbonate system in the
536 full salinity and temperature spectrum of sea ice brines.
537

538 **4. Conclusions**

539 The stoichiometric dissociation constants of carbonic acid determined in this study extended
540 the existing oceanographic data set to below-zero temperatures and salinities greater than 50 to
541 the freezing point of salinity 100 brines with major ionic composition and major ionic ratios
542 equivalent to those of reference seawater. They are reported here in the total proton scale and
543 each is fitted to a salinity and temperature function for interpolation in sea ice brine investigations

544 of the internal carbonate system of the medium. This work confirmed the uncertainties of the
545 salinity and temperature extrapolation of the existing oceanographic functions for application
546 outside their empirical ranges. There were also indications for uncertainty in the current state of
547 knowledge of the thermodynamic parameters (e.g., total activity coefficient of the carbonate ion)
548 for the second dissociation constant of carbonic acid at below-zero temperatures. Further relevant
549 work is thus needed for accurate parameterization of the carbonate ion interactions with the
550 remainder of sea solutes in brines at below-zero temperatures and for the dissociation constants
551 of carbonic acid in the coldest temperature and salinity range of non-conservative oceanic brines
552 at equilibrium with authigenic cryogenic minerals to the eutectic of seawater.
553

554 **Acknowledgements**

555 This work was supported by a NERC-UK grant (grant NE/J011096/1). We thank Susan
556 Allender for the dissolved macro-nutrient analyses and Dr. Ben Butler for the analyses of the
557 major ions in the experimental solutions.
558

559 **References**

560 Arrigo K. R., Worthen D. L., Lizotte M. P., Dixon P. and Dieckmann G. S. (1997) Primary
561 production in Antarctic sea ice. *Science* **276**, 394-397.
562 Assur A. (1958) Composition of sea ice and its tensile strength in Arctic sea ice. U. S. National
563 Academy of Sciences, National Research Council, Publ. 598, 106-138.
564 Barford N. C. (1985) Experimental measurements: Precision, error, and truth. John Wiley &
565 Sons, Chichester, UK.
566 Bockmon E. E. and Dickson A. G. (2015) An inter-laboratory comparison assessing the quality
567 of seawater carbon dioxide measurements. *Mar. Chem.* **171**, 36-43.
568 Brown K. A., Miller L. A., Davelaar M., Francois R. and Tortell P.D. (2014) Over-determination
569 of the carbonate system in natural sea-ice brine and assessment of carbonic acid dissociation
570 constants under low temperature, high salinity conditions. *Mar. Chem.* **165**, 36-45.
571 Butler B. M. and Kennedy H. (2015) An investigation of mineral dynamics in frozen seawater
572 brines by direct measurement with synchrotron X-ray powder diffraction. *J. Geophys. Res. Oceans* **120**, 5686-5697, doi:10.1002/2015JC011032.

574 Butler B. M., Papadimitriou S., Santoro A., Kennedy H. (2016) Mirabilite solubility in
575 equilibrium sea ice brines. *Geochim. Cosmochim. Acta* **182**, 40-54.
576 Cai W.-J., Chen L., Chen B., Gao Z., Lee S. H., Chen J., Pierrot D., Sullivan K., Wang Y., Hu X.,
577 Huang W.-J., Zhang Y., Xu S., Murata A., Grebmeier J. M., Jones E. P. and Zhang H. (2010)
578 *Science* **329**, 556-559.
579 Caldeira K. and Wickett M. E. (2003) Anthropogenic carbon and ocean pH. *Nature* **425**, 365.
580 Crowley T. J. (2000) Causes of climate change over the past 1000 years. *Science* **289**, 270-277.
581 Delille B., Jourdain B., Borges A. V., Tison J.-L. and Delille D. (2007) Biogas (CO_2, O_2,
582 dimethylsulfide) dynamics in spring Antarctic fast ice. *Limnol. Oceanogr.* **52**, 1367-1379.
583 Delille B., Vancoppenolle M., Geilfus N.-X., Tilbrook B., Lannuzel D., Schoemann V.,
584 Becquevort S., Carnat G., Delille D., Lancelot C., Chou L., Dieckmann G. S. and Tison J.-L.
585 (2014) Southern ocean CO_2 sink: The contribution of the sea ice. *J. Geophys. Res. Oceans*
586 **119**, 6340-6355.
587 Dickson A. G. (1990) Thermodynamics of the dissociation of boric acid in synthetic seawater
588 from 273.15 to 318.15 K. *Deep-Sea Res.* **37**, 755-766.
589 Dickson A. G. and Millero F. J. (1987) A comparison of the equilibrium constants for the
590 dissociation of carbonic acid in seawater media. *Deep-Sea Res.* **34**, 1733-1743.
591 Dickson A. G., Sabine C. L. and Christian J. R. (Eds.) (2007) Guide to best practices for ocean
592 CO_2 measurements. PICES Special Publication 3, 191 pp.
593 Dieckmann G. S., Nehrke G., Papadimitriou S., Göttlicher J., Steininger R., Kennedy H., Wolf-
594 Gladrow D. and Thomas D. N. (2008) Calcium carbonate as ikaite crystals in Antarctic sea
595 ice. *Geophys. Res. Lett.* **35**, L08501, doi:10.1029/2008GL033540.
596 Feely R. A., Sabine C. L., Lee K., Berelson W., Kleypas J., Fabry V. J., Millero F. J. (2004)
597 Impact of anthropogenic CO_2 on the $CaCO_3$ system in the oceans. *Science* **305**, 362-366.
598 Feely R. A., Sabine C. L., Hernandez-Ayon J. M., Janson D. and Hales B. (2008) Evidence for
599 upwelling of corrosive "acidified" water onto the continental shelf. *Science* **320**, 1490-1492.
600 Fischer M., Thomas D. N., Krell A., Nehrke G., Göttlicher J., Norman L., Meiners K. M., Riaux-
601 Gobin C. and Dieckmann G. S. (2013) Quantification of ikaite in Antarctic sea ice. *Antarct.*
602 *Sci.* **25**, 421-432.
603 Fransson A., Chierici M., Yager P. L. and Smith Jr. W. O. (2011) Antarctic sea ice carbon
604 dioxide system and controls. *J. Geophys. Res.* **116**, C12035, doi:10.1029/2010JC006844.

605 Fritsen C. H., Lytle V. I., Ackley S. F. and Sullivan C. W. (1994) Autumn bloom of Antarctic
606 pack–ice algae. *Science* **266**,782-784.
607 Gattuso J.-P., Magnan A., Billé R., Cheung W. W. L., Howes E. L., Joos F., Allemand D., Bopp
608 L., Cooley S. R., Eakin C. M., Hoegh-Guldberg O., Kelly R. P., Pörtner H.-O., Rogers A. D.,
609 Baxter J. M., Laffoley D., Osborn D., Rankovic A., Rochette J., Sumaila U. R., Treyer S. and
610 Turley C. (2015) Contrasting futures for ocean and society from different anthropogenic CO_2
611 emissions scenarios. *Science* **349**, 45, http://dx.doi.org/10.1126/science.aac4722.
612 Geilfus N. X., Carnat G., Papakyriakou T. N., Tison J.-L., Else B., Thomas H., Shadwick E. and
613 Delille B. (2012a) Dynamics of pCO_2 and related air-ice CO_2 fluxes in the Arctic coastal zone
614 (Amundsen Gulf, Beaufort Sea). *J. Geophys. Res.* **117**, C00G10, doi:10.1029/2011JC007118.
615 Geilfus N. X., Delille B., Verbeke V. and Tison J.-L. (2012b) Towards a method for high vertical
616 resolution measurements of the partial pressure of CO_2 within bulk sea ice. *J. Glaciol.* **58**,
617 208-212.
618 Gleitz M., v.d. Loeff M. R., Thomas D. N., Dieckmann G. S. and Millero F. J. (1995)
619 Comparison of summer and winter inorganic carbon, oxygen and nutrient concentrations in
620 Antarctic sea ice brine. *Mar. Chem.* **51**, 81-91.
621 Golden K. M., Ackley S. F. and Lytle V. I. (1998) The percolation phase transition in sea ice.
622 *Science* **282**, 2238-2241.
623 Goyet C. and Poisson A. (1989) New determination of carbonic acid dissociation constants in
624 seawater as a function of temperature and salinity. *Deep-Sea Res.* **36**, 1635-1654.
625 Hales B., Chipman D. and Takahashi T. (2004a) High-frequency measurements of partial
626 pressure and total concentration of carbon dioxide in seawater using microporous hydrophobic
627 membrane contactors. *Limnol. Oceanogr. Methods* **2**, 356-364.
628 Hales B., van Greer A. and Takahashi T. (2004b) High-frequency measurements of seawater
629 chemistry: Flow-injection analysis of macronutrients. *Limnol. Oceanogr. Methods* **2**, 91-101.
630 Hain M. P., Sigman D. M., Higgins J. A. and Haug G. H. (2015) The effects of secular calcium
631 and magnesium concentration changes on the thermodynamics of seawater acid/base
632 chemistry: Implications for Eocene and Cretaceous ocean carbon chemistry and buffering.
633 *Global Biogeochem. Cycles* **29**, 517-533.
634 Hansson I. (1973) A new set of acidity constants for carbonic acid and boric acid in seawater.
635 *Deep-Sea Res.* **20**, 461-478.

He S. and Morse J. W. (1993) The carbonic acid system and calcite solubility in aqueous Na-K-Ca-Mg-Cl-SO_4 solutions from 0 to 90°C. *Geochim. Cosmochim. Acta* **57**, 3533-3554.

Howarth R. W. (1978) A rapid and precise method for determining sulfate in seawater, estuarine waters, and sediment pore waters. *Limnol. Oceanogr.* **23**, 1066-1069.

Kennedy H., Thomas D. N., Kattner G., Haas C. and Dieckmann G. S. (2002) Particulate organic matter in Antarctic summer sea ice: concentration and stable isotopic composition. *Mar. Ecol. Prog. Ser.* **238**, 1-13.

Lee K., Kim T.-W., Byrne R. H., Millero F. J., Feely R. A. and Liu Y.-M. (2010) The universal ratio of boron to chlorinity for the North Pacific and North Atlantic oceans. *Geochim. Cosmochim. Acta* 74, 1801-1811.

Liu X., Patsavas M. C. and Byrne R. H. (2011) Purification and characterization of meta-Cresol Purple for spectrophotometric seawater pH measurements. *Environ. Sci. Technol.* 45, 4862-4868.

Loucaides S., Rérolle V. M. C., Papadimitriou S., Kennedy H., Mowlem M. C., Dickson A. G., Gledhill M. and Achterberg E. P. (2017) Characterization of *meta*-Cresol Purple for spectrophotometric pH measurements in saline and hypersaline media at sub-zero temperatures. Accepted in *Scientific Reports.*

Lueker T. J., Dickson A. G. and Keeling C. D. (2000) Ocean pCO_2 calculated from dissolved inorganic carbon, alkalinity, and equations for K_1 and K_2: validation based on laboratory measurements of CO_2 in gas and seawater at equilibrium. *Mar. Chem.* 70, 105-119.

Marion G. M. (2001) Carbonate mineral solubility at low temperatures in the Na-K-Mg-Ca-H-Cl-SO_4-OH-HCO_3-CO_3-CO_2-H_2O system. *Geochim. Cosmochim. Acta* **65**, 1883–1896.

Marion G. M., Mironenko M. V. and Roberts M. W. (2010) FREZCHEM: A geochemical model for cold aqueous solutions. *Comput. Geosci.* **36**, 10-15.

Mehrbach C., Culberson C. H., Hawley J. E. and Pytkowicz R. M. (1973) Measurement of the apparent dissociation constants of carbonic acid in seawater at atmospheric pressure. *Limnol. Oceanogr.* **18**, 897-907.

Miller L. A., Fripiat F., Else B. G. T., Bowman J. S., Brown K. A., Collins R. E., Ewert M., Fransson A., Gosselin M., Lannuzel D., Meiners K. M., Michel C., Nishioka J., Nomura D., Papadimitriou S., Russell L. M., Sørensen L. L., Thomas D. N., Tison J.-L., van Leeuwe M. A., Vancoppenolle M., Wolff E.W., Zhou J. (2015) Methods for biogeochemical studies of sea

667 ice: The state of the art, caveats, and recommendations. *Elementa: Science of the*
668 *Anthropocene* **3**, 000038, doi: 10.12952/journal.elementa.000038.
669 Miller L. A., Carnat G., Else B. G. T., Sutherland N. and Papakyriakou T. N. (2011a) Carbonate
670 system evolution at the Arctic Ocean surface during autumn freeze-up. *J. Geophys. Res.* **116**,
671 C00G04, doi: 10.1029/2011JC007143.
672 Miller L. A., Papakyriakou T. N., Collins R. E., Deming J. W., Ehn J. K., Macdonald R. W.,
673 Mucci A., Owens O., Raudsepp M. and Sutherland N. (2011b) Carbon dynamics in sea ice: A
674 winter flux time series. *J. Geophys. Res.* **116**, C02028, doi: 10.1029/2009JC006058.
675 Millero F. J. (1995) Thermodynamics of the carbon dioxide system in the oceans. *Geochim.*
676 *Cosmochim. Acta* **59**, 661–677.
677 Millero F. J. and Huang F. (2009) The density of seawater as a function of salinity (5 to 70 g kg^{-1})
678 and temperature (273.15 to 363.15 K). *Ocean Sci.* **5**, 91-100.
679 Millero, F.J., Zhang, J.Z., Fiol, S., Sotolongo, S., Roy, R.N., Lee K., Mane S. (1993) The use of
680 buffers to measure the pH of seawater. *Mar. Chem.* **44**, 143-152.
681 Millero F. J., Pierrot D., Lee K., Wanninkhof R., Feely R., Sabine C. L., Key R. M. and
682 Takahashi T. (2002) Dissociation constants for carbonic acid determined from field
683 measurements. *Deep-Sea Res. Part I* **49**, 1705-1723.
684 Millero F. J., Graham T. B., Huang F., Bustos-Serrano H. and Pierrot D. (2006) Dissociation
685 constants of carbonic acid in seawater as a function of salinity and temperature. *Mar. Chem.*
686 **100**, 80-94.
687 Millero F. J., Feistel R., Wright D. G. and McDougall T. J. (2008) The composition of standard
688 seawater and the definition of the reference-composition salinity. *Deep-Sea Res Part I* **55**, 50-
689 72.
690 Mohica-Prieto F. J. and Millero F. J. (2002) The values of $pK_1 + pK_2$ for the dissociation of
691 carbonic acid in seawater. *Geochim. Cosmochim. Acta* **66**, 2529–2540.
692 Munro D. R., Dunbar R. B., Mucciarone D. A., Arrigo K. R. and Long M. C. (2010) Stable
693 isotopic composition of dissolved inorganic carbon and particulate organic carbon in sea ice
694 from the Ross Sea, Antarctica. *J. Geophys. Res.* **115**, C09005, doi:10.1029/2009JC005661.
695 Papadimitriou S., Kennedy H., Kattner G., Dieckmann G. S. and Thomas D. N. (2004)
696 Experimental evidence for carbonate precipitation and CO_2 degassing during sea ice
697 formation. *Geochim. Cosmochim. Acta* **68**, 1749-1761.

Papadimitriou S., Thomas D. N., Kennedy H., Haas C., Kuosa H., Krell H. and Dieckmann D. S. (2007) Biogeochemical composition of natural sea ice brines from the Weddell Sea during early austral summer. *Limnol. Oceanogr.* **52**, 1809-1823.

Papadimitriou S., Kennedy H., Norman L., Kennedy D. P. and Thomas D. N. (2012) The effect of biological activity, $CaCO_3$ mineral dynamics, and CO_2 degassing in the inorganic carbon cycle in sea ice in late winter-early spring in the Weddell Sea, Antarctica. *J. Geophys. Res.* **117**, C08011, doi: 10.1029/2012JC008058.

Papadimitriou S., Kennedy H., Kennedy P. and Thomas D. N. (2013) Ikaite solubility in seawater-derived brines at 1 atm and sub-zero temperatures to 265 K. *Geochim. Cosmochim. Acta* **109**, 241-253, doi:10.1016/j.gca.2013.01.044.

Papadimitriou S., Kennedy H., Kennedy P. and Thomas D. N. (2014) Kinetics of ikaite precipitation and dissolution in seawater-derived brines at subzero temperatures to 265 K. *Geochim. Cosmochim. Acta* **140**, 199-211, doi: 10.1016/j.gca.2014.05.031.

Papadimitriou S., Loucaides S., Rérolle V. M. C., Achterberg E. P., Dickson A. G., Mowlem M. C. and Kennedy H. (2016) The measurement of pH in saline and hypersaline media at sub-zero temperatures: Characterization of Tris buffers. *Mar. Chem.***184**, 11-20.

Pierrot D., Neill C., Sullivan K., Castle R., Wanninkhof R., Lüge H., Johannessen T., Olsen A., Feely R. A. and Cosca C. E. (2009) Recommendations for autonomous underway pCO_2 measuring systems and data reduction techniques. *Deep-Sea Res Part II* **56**, 512-522.

Pitzer K. S. (1973) Thermodynamics of electrolytes. I. Theoretical basis and general equations. *J. Phys. Chem.* **77**, 268–277.

Plummer N. L. and Busenberg E. (1982) The solubility of calcite, aragonite, and vaterite in CO_2-water solutions between 0 – 90 °C and an evaluation of the aqueous model for the system CO_2-H_2O-$CaCO_3$. *Geochim. Cosmochim. Acta* **46**, 1011-1040.

Pytkowicz R. M. and Kester D. R. (1969) Harned's rule behaviour of NaCl–Na_2SO_4 solutions explained by an ion association model. *Am. J. Sci.* **267**, 217–229.

Rérolle V. M. C., Floquet C. F. A., Harris A. J. K., Mowlem M. C., Bellerby R. R. G. J. and Achterberg E. P. (2013) Development of a colorimetric microfluidic pH sensor for autonomous seawater measurements. *Anal. Chim. Acta* **786**, 124-131.

Roy R. N., Roy L. N., Lawson M., Vogel K. M., Porter-Moore C., Davis W., Millero F. J. and Campbell D. M. (1993) The dissociation constants of carbonic acid in seawater at salinities 5 to 45 and temperatures 0 to 45 °C. *Mar. Chem.* **44**, 249-259.

Rysgaard S., Glud R. N., Sejr M. K., Bendtsen J. and Christensen P. B. (2007) Inorganic carbon transport during sea ice growth and decay: A carbon pump in polar seas. *J. Geophys. Res. Oceans* **112**, C03016, doi: 10.1029/2006JC003572.

Rysgaard S., Bendtsen J., Delille B., Dieckmann G. S., Glud R. N., Kennedy H., Mortensen J., Papadimitriou S., Thomas D. N. and Tison J.-L. (2011) Sea ice contribution to the air–sea CO_2 exchange in the Arctic and Southern Oceans. *Tellus B* **63**, 823-830.

Sabine C. L., Feely R. A., Gruber N., Key R. M., Lee K., Bullister J. L., Wanninkhof R., Wong C. S., Wallace D. W. R., Tilbrook B., Millero F. J., Peng T.-H., Kozyr A., Ono T., Rios A. F. (2004) The oceanic sink for anthropogenic CO_2. *Science* **305**, 367-371.

Semiletov I., Pipko I., Gustafsson Ö., Anderson L. G., Sergienko V., Pugach S., Dudarev O., Charkin A., Gukov A., Bröder L., Andersson A., Spivak E. and Shakhova N. (2016) Acidification of East Siberian Arctic Shelf waters through addition of freshwater and terrestrial carbon. *Nat. Geosci.* **9**, 361-365.

Takahashi T. (2004) The fate of industrial carbon dioxide. *Science* **305**, 352-353.

Takahashi T., Sutherland S. C., Chipman D. W., Goddard J. G., Ho C., Newberger T., Sweeney C. and Munro D. R. (2014) Climatological distributions of pH, pCO_2, total CO_2, alkalinity, and $CaCO_3$ saturation in the global surface ocean, and temporal changes at selected locations. *Mar. Chem.* **164**, 95-125.

Takahashi T., Feely R. A., Weiss R. F., Wanninkhof R. H., Chipman D. W., Sutherland S. C. and Takahashi T. T. (1997) Global air-sea flux of CO_2: An estimate based on measurements of sea-air pCO_2 difference. *Proc. Natl.Acad. Sci. USA* **94**, 8292-8299.

Thomas D. N. and Dieckmann G. S. (2002) Sea ice – A habitat for extremophiles. *Science* **295**, 641-644.

Turner D. R., Achterberg E. P., Chen C.-T. A., Clegg S. L., Hatje V., Maldonado M., Sander S. G., van den Berg C. M. G. and Wells M. (2016) Toward a quality-controlled and accessible Pitzer model for seawater and related systems. *Front. Mar. Sci.* **3**, 139, doi:10.3389/fmars.2016.00139.

757 UNESCO 1983. Algorithms for computation of fundamental properties of seawater. Unesco
758 Technical Papers in Marine Science 44, 53 pp.
759 Weiss R. S. (1974) Carbon dioxide in water and seawater: The solubility of a non-ideal gas. *Mar.*
760 *Chem.* **2**, 203-215.
761 Yamamoto-Kawai M., McLaughlin F. A., Carmack E. C., Nishino S. and Shimada K. (2009)
762 Aragonite undersaturation in the Arctic Ocean: Effects of ocean acidification and sea ice melt.
763 *Science* **326**, 1098-1100.
764
765
766

List of Figures

Figure 1. The stoichiometric first and second dissociation constants of carbonic acid as negative common logarithm versus temperature (open circles) in natural seawater (S_P = 33 – 34). The curves were derived from the salinity-temperature functions in Lueker et al. (2000) based on the measurements of Mehrbach et al. (1973) (dashed line) and from the measurements on the seawater proton scale of Millero et al. (2006), converted to the total proton scale as in Millero (1995) and re-fitted here (solid line). Note the difference in the scale of the *y*-axis in the pK^*_{1C} and pK^*_{2C} panels.

Figure 2. The stoichiometric first and second dissociation constants of carbonic acid as negative common logarithm versus salinity from this study (open circles) and from Millero et al. (2006) (crosses) when available at 20 °C [panels (a) and (b)], 5 °C [panels (c) and (d)], 0 °C [panels (e) and (f)], and the freezing point [panels (g) and (h)]. The dashed curve represents the salinity-temperature functions in Lueker et al. (2000) based on the measurements of Mehrbach et al. (1973), extrapolated outside their empirical range of S_P = 19 – 43 and for t < 2.0 °C. The solid curve represents the salinity-temperature functions based on the measurements on the seawater proton scale of Millero et al. (2006), converted to the total proton scale and re-fitted here, and extrapolated outside their empirical range for S_P > 51 and for t < 1.0 °C. Note the difference in the scale of the *y*-axis in the pK^*_{1C} and pK^*_{2C} panels.

Figure 3. The stoichiometric first and second dissociation constants of carbonic acid as negative common logarithm versus temperature at the freezing point of seawater-derived brine from this study (open circles) and from the output of the thermodynamic code FREZCHEM v15.1 (dashed line). Note the equivalent scale of the *y*-axis in the pK^*_{1C} and pK^*_{2C} panels.

Figure 4. Difference between observed and fitted values of the first and second dissociation constants of carbonic acid in seawater and brines as a function of salinity [panels (a) and (b)] and temperature [panels (c) and (d)].

Figure 5. Change in pH in the total proton scale [panels (a), (d)], CO_2 fugacity [panels (b), (e)], and the total concentration of the carbonate ion [panels (c), (f)] in sea ice brine inclusions at ice-brine equilibrium (freezing point) as a function temperature in conservative seawater-derived brines with respect to major ionic composition, A_T, and C_T (upper panels), and in conservative brines at equilibrium with current atmospheric CO_2 (non-conservative C_T) (lower panels). The

values of the illustrated parameters were determined for equilibrium freezing of surface seawater from the western Weddell Sea, Antarctica, in Papadimitriou et al. (2012) by solving the system of equations that describe the chemical equilibria of the marine CO_2 system using the dissociation constants of carbonic acid from this study (solid line), and as computed from the salinity-temperature functions fitted to the measurements of Mehrbach et al. (1973) by Lueker et al. (2000) (dashed line) and to the measurements of Millero et al. (2006) following conversion to the total proton scale and re-fitting in this study (dotted line). Further details are given in *Section 2.7*.

807 **Table 1.** Major ion composition of brines (in mmol kg^{-1}).

Salinity	$[Na^+]$	$[Mg^{2+}]$	$[Ca^{2+}]$	$[K^+]$	$[Cl^-]$	$[SO_4^{2-}]$
100.52	1347	150.64	29.96	25.85	1566	77.21
98.69	1323	148.89	28.99	26.26	1554	77.47
84.62	1134	128.02	25.00	22.26	1327	66.97
61.54	825	92.66	18.18	16.23	968	50.48
60.30	808	91.34	17.87	15.40	946	47.25
60.28	808	91.25	17.84	16.11	944	47.93
50.24	681	74.20	14.54	13.57	795	39.79
50.15		75.15	14.55			40.37
48.90		72.65	14.30			38.80
40.20	539	60.84	11.83	11.09	632	32.77
[a]35	470±2	52.60±0.45	10.29±0.10	9.27±0.23	550±2	27.82±0.54
[b]35	469	52.82	10.28	10.21	546	28.24

808 [a]mean concentration of brines normalized to salinity 35

809 [b]reference composition for seawater of salinity 35 (Millero et al., 2008)

810

811 **Table 2.** Practical salinity (S_P), temperature (*t*, in °C), phosphate (SRP) and silicic acid [$Si(OH)_4$]
812 (in μmol kg^{-1}), the measured parameters of the carbonate system in seawater and seawater-
813 derived brines [C_T (in μmol kg^{-1}), A_T and derived carbonate alkalinity (A_C) (in μmol kg^{-1}), fCO_2
814 (in μatm), and pH_T (total proton scale; in mol kg^{-1})], and the stoichiometric first and second
815 dissociation constants of carbonic acid (in mol kg^{-1}, total proton scale) as negative common
816 logarithms (pK^*_{1C} and pK^*_{2C}).

S_P	SRP	$Si(OH)_4$	*t*	C_T	A_T	A_C	fCO_2	pH_T	pK^*_{1C}	pK^*_{2C}
33.14	0.1	2.9	–1.79	2047	2259	2177	184	8.345	6.167	9.468
33.54	0.0	8.1	17.98	2042	2282	2200	369	8.052	5.889	9.089
33.64	0.3	3.8	–1.53	2153	2287	2231	329	8.125	6.163	9.432
			–1.53	2157	2287	2231	329	8.122	6.158	9.448
			–1.53	2154	2287	2232	331	8.118	6.158	9.425
			22.01	2139	2287	2233	788	7.780	5.866	9.007
33.64	0.3	3.8	15.07	2114	2281	2221	520	7.934	5.932	9.126
			15.07	–	2281	2221	519	7.929	–	–
			15.11	2119	2281	2220	518	7.935	5.928	9.151
			25.01	2144	2281	2229	887	7.731	5.832	8.991
			25.02	2138	2281	2228	872	7.737	5.833	8.977
			25.06	2141	2281	2228	880	7.732	5.830	8.984
33.94	0.0	7.1	–1.17	2063	2278	2194	186	8.333	6.143	9.457
			–1.06	2073	2278	2199	206	8.298	6.148	9.436
			–1.06	–	2278	2199	203	8.298	–	–
			–0.03	2045	2278	2192	186	8.329	6.127	9.401
			0.04	2064	2278	2194	201	8.309	6.132	9.435
			0.04	2061	2278	2195	202	8.308	6.135	9.420
			0.04	2061	2278	2195	201	8.305	6.130	9.418
			5.03	2050	2278	2195	237	8.232	6.052	9.309
			9.94	2048	2278	2198	280	8.148	5.968	9.210
			20.04	2044	2278	2202	433	7.986	5.866	9.019
			24.96	2100	2278	2213	676	7.835	5.831	9.003
			24.99	2100	2278	2214	682	7.832	5.832	8.996
			25.04	2091	2278	2213	680	7.833	5.835	8.968
34.04	0.2	4.8	0.00	2053	2286	2199	191	8.327	6.134	9.403
			0.00	2054	2286	2199	190	8.324	6.128	9.403
			0.00	–	2286	2199	191	8.323	–	–
			0.06	2049	2286	2195	181	8.350	6.133	9.427
			20.03	2050	2286	2206	430	8.005	5.880	9.045
			20.03	2048	2286	2206	420	8.004	5.870	9.039
			20.03	2048	2286	2206	427	8.004	5.877	9.039

817

818

819 **Table 2** (continued)

S_P	SRP	$Si(OH)_4$	*t*	C_T	A_T	A_C	fCO_2	pH_T	pK^*_{1C}	pK^*_{2C}
40.20	0.1	46.9	–2.15	2512	2806	2703	216	8.327	6.123	9.375
			4.97	2584	2806	2729	426	8.071	6.025	9.229
48.90	0.0	259.4	–2.72	3177	3528	3411	347	8.247	6.134	9.300
			-0.09	3155	3528	3413	385	8.198	6.092	9.206
			20.05	3142	3528	3420	851	7.883	5.841	8.850
50.15	0.0	55.2	–2.74	3026	3481	3329	224	8.397	6.123	9.326
			–2.74	3038	3481	3337	248	8.366	6.134	9.300
50.24	0.0	38.3	–1.56	2947	3446	3296	232	8.373	6.114	9.223
			–0.06	2976	3446	3306	268	8.312	6.082	9.191
			4.88	2976	3446	3308	329	8.233	6.013	9.109
			10.00	2944	3446	3306	383	8.168	5.949	8.998
			15.00	2984	3446	3318	532	8.051	5.896	8.921
			25.05	2977	3446	3323	807	7.895	5.807	8.743
60.28	0.4	15.3	–3.36	3645	4116	3965	379	8.284	6.137	9.264
			–0.27	3643	4116	3968	419	8.229	6.073	9.202
			25.02	3627	4116	3987	1183	7.802	5.765	8.718
60.30	1.2	26.9	–3.37	3641	4180	4012	302	8.340	6.101	9.259
			–2.40	3652	4180	4016	308	8.310	6.060	9.240
			–2.37	3661	4180	4016	318	8.308	6.069	9.250
			20.29	3649	4180	4035	864	7.925	5.802	8.819
61.54	0.4	0.5	–3.46	3707	4228	4060	328	8.331	6.115	9.279
			–0.11	3705	4228	4062	370	8.276	6.056	9.219
84.62	1.0	18.0	–4.97	4863	5811	5562	371	8.409	6.118	9.167
			–4.93	4842	5811	5560	366	8.413	6.120	9.155
			0.04	4840	5811	5567	455	8.318	6.035	9.054
			5.02	4855	5811	5579	583	8.216	5.960	8.954
			20.33	4847	5811	5599	1088	7.953	5.773	8.668
98.69	1.4	22.6	–6.00	5457	6795	6486	392	8.509	6.196	9.130
			–5.93	5454	6795	6483	356	8.512	6.156	9.134
			0.03	5459	6795	6498	459	8.390	6.042	9.007
			4.87	5441	6795	6504	546	8.304	5.960	8.907
100.52	2.0	20.7	–5.98	5628	6901	6611	417	8.469	6.157	9.129
			20.30	5656	6901	6673	1308	7.946	5.755	8.587

820

821

Table 3. Best fit values for the coefficients of the salinity-temperature functions of the first and second stoichiometric dissociation constants of carbonic acid in seawater and seawater-derived brines on the total proton scale.

		data set			
		Millero et al. (2006)		this study	
Parameter	Coefficient	pK^*_{1C}	pK^*_{2C}	pK^*_{1C}	pK^*_{2C}
$S_P^{0.5}$	a_o	13.76048	21.070728	6.14528	27.557655
S_P	a_1	0.0326145	0.1232366	–0.127714	0.154922
S_P^2	a_2	$–5.5709\times10^{–5}$	$–3.68\times10^{–4}$	$7.396\times10^{–5}$	$–2.48396\times10^{–4}$
$S_P^{0.5}$ /T	a_3	–547.407	–774.949	–622.886	–1014.819
S_P/T	a_4	–5.912	–19.5887	29.714	–14.35223
$S_P^{0.5}$ lnT	a_5	–2.118981	–3.328493	–0.666812	–4.4630415
constant	b_o	[a] –126.34048	[a] –90.18333	–176.48	–323.52692
1/T	b_1	[a] 6320.813	[a] 5143.692	9914.37	14763.287
lnT	b_2	[a] 19.568224	[a] 14.613358	26.05129	50.385807
user confirmation value S_P = 35, T = 273.15 K		6.1182	9.3827	6.1267	9.3940

[a] from Millero et al. (2006)

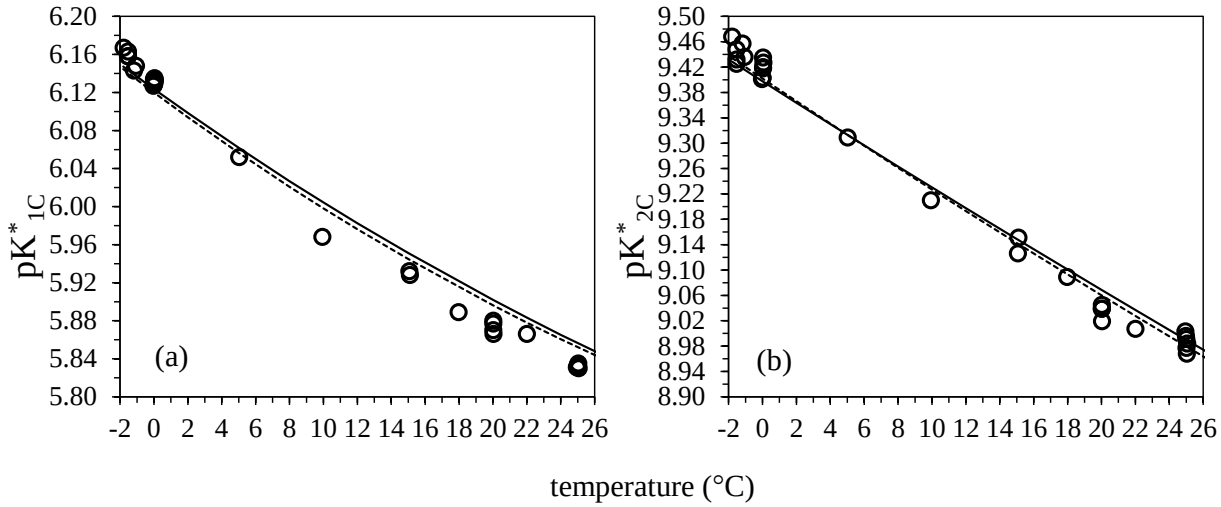

Figure 1
Papadimitriou et al.

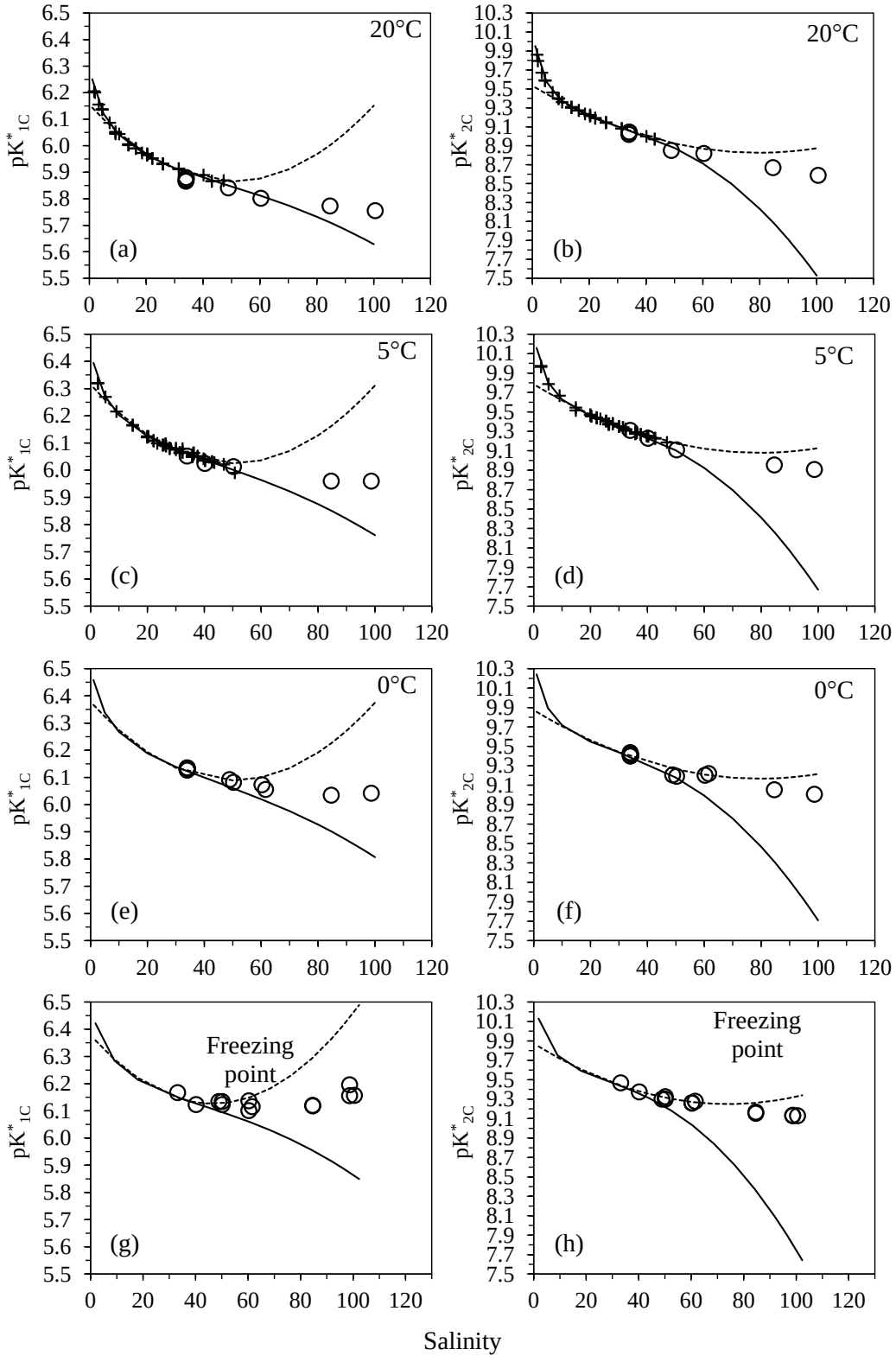

Figure 2
Papadimitriou et al.

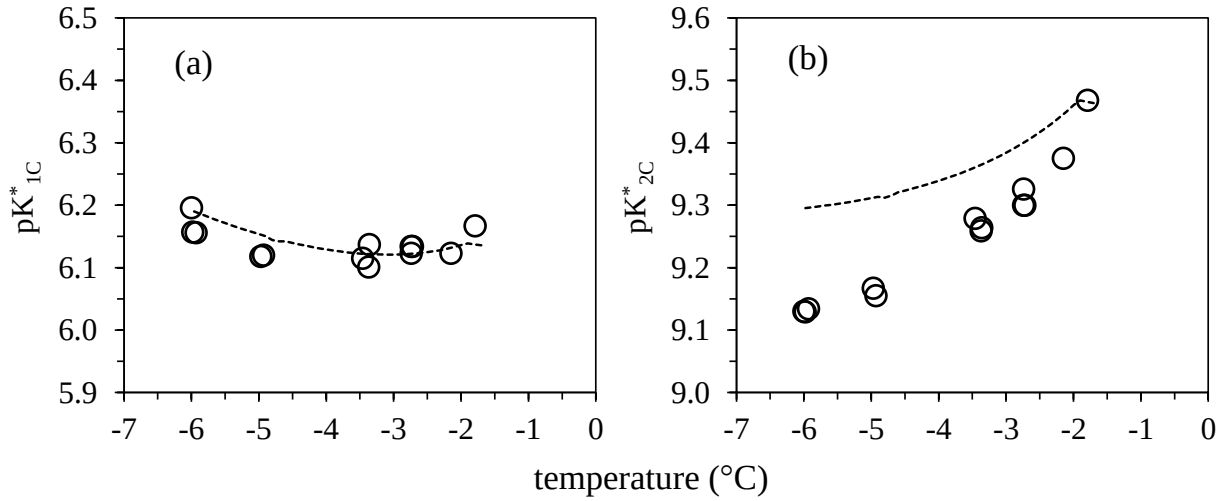

Figure 3
Papadimitriou et al.

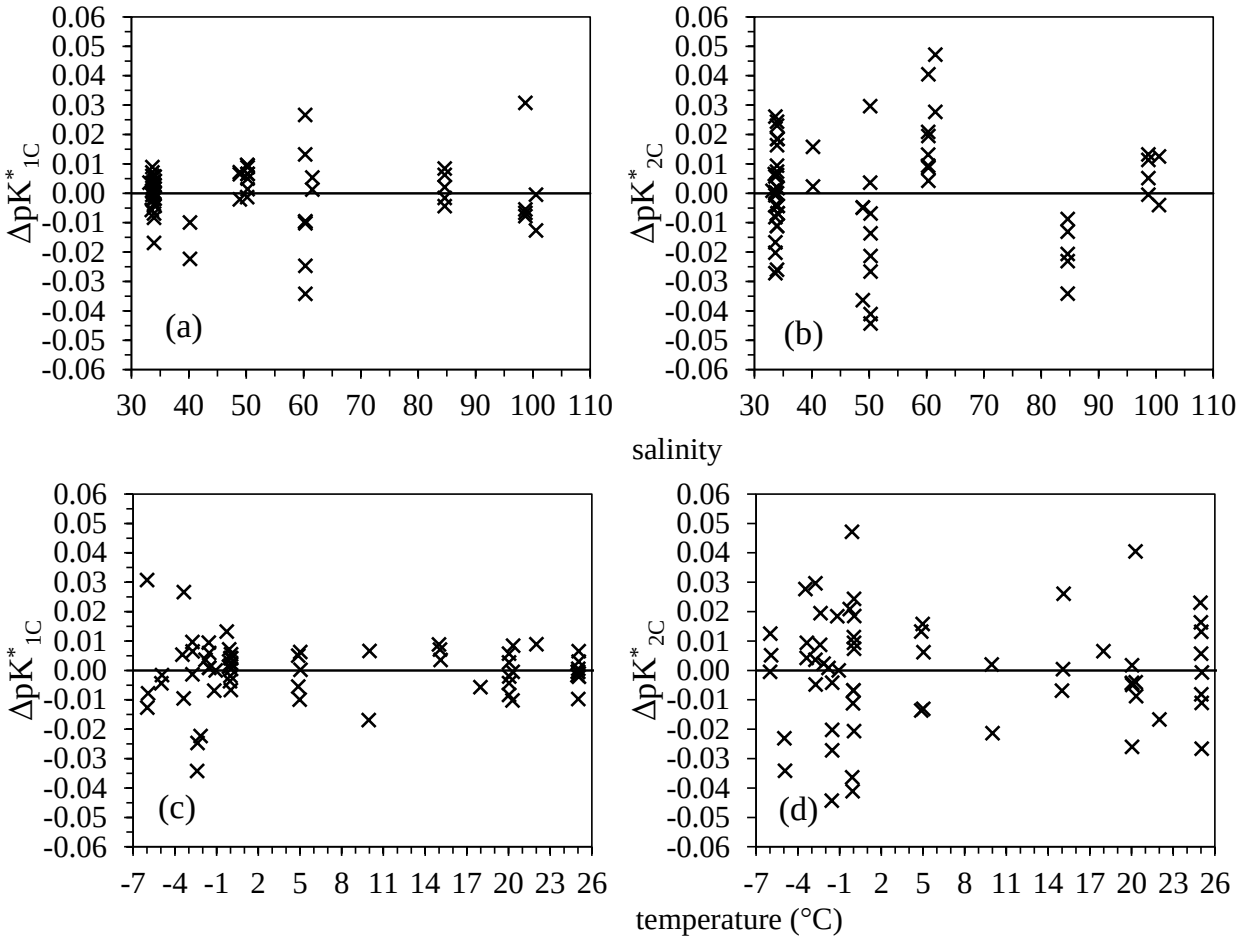

Figure 4
Papadimitriou et al.

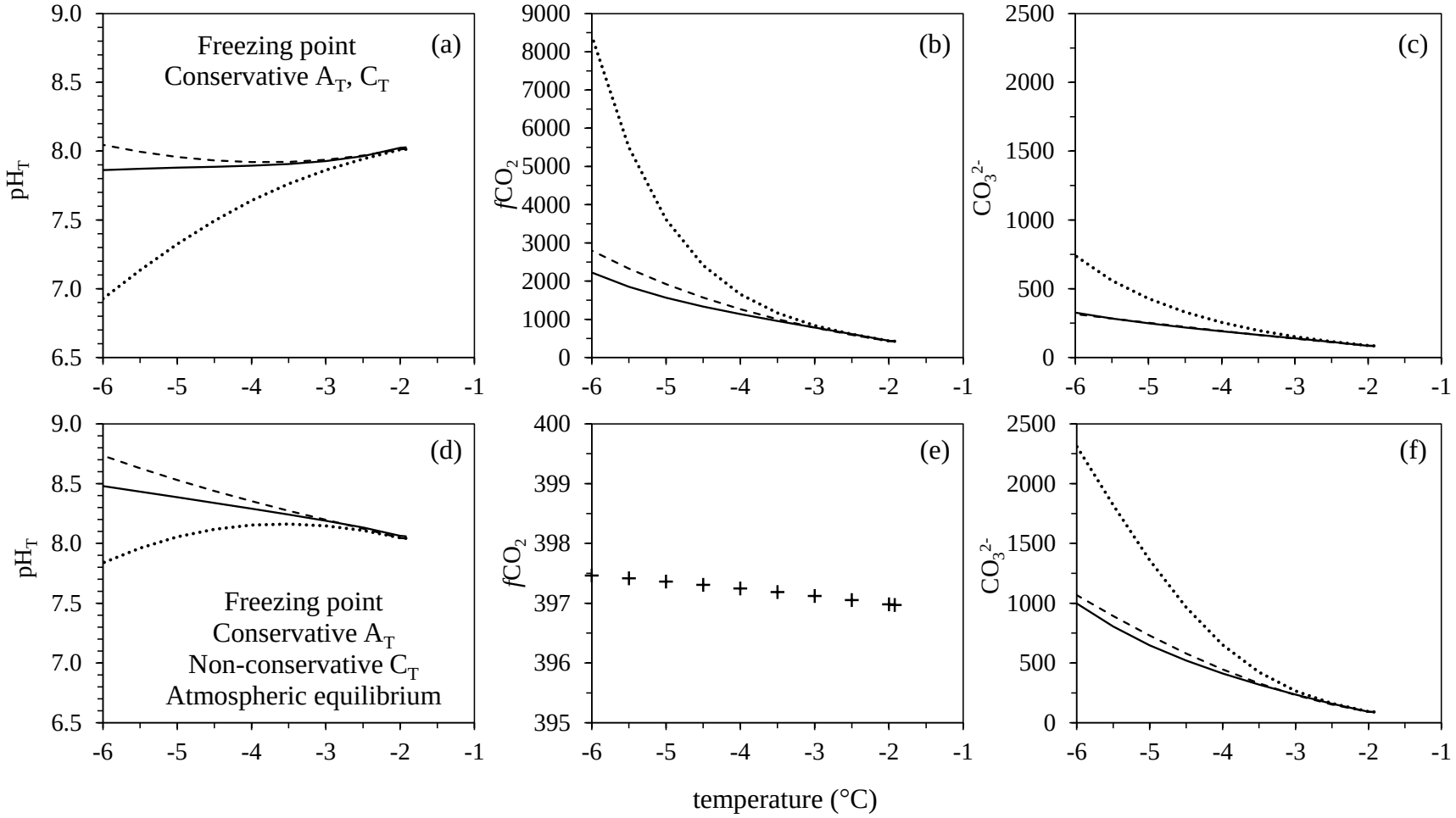

Figure 5
Papadimitriou et al.